Heimo Tuovinen and Margaret Simonson

Incorporation of Detailed Chemistry into CFD Modelling of Compartments Fires

SP Swedish National Testing and Research Institute
Fire Technology
SP REPORT 1999:03

Heimo Tuovinen and Margaret Simonson

Incorporation of Detailed Chemistry into CFD Modelling of Compartments Fires

SP Swedish National Testing and Research Institute
Fire Technology
SP REPORT 1999:03

Abstract

Flamelet calculation for heptane, propane and methane with and without fire gas re-circulation have been made. The calculations are performed using so called Arclength Continuation Method, in which a system of differential equations is solved by including the inverse of the scalar dissipation rate as a variable. The calculations are based on 2000 elementary reaction steps involving more than 100 species. The flamelets for both cold (300 K) and hot (1000 K) combustion product re-circulation have been calculated. The strain is also included in the calculation; also the scalar dissipation rates from 0.01/s to extinction values have been varied.

From this main data base the flamelet library for heptane has been made, which can be sourced directly by the CFD code SOFIE. Only the major species, O_2, H_2O, CO, CO_2, N_2 and fuel are taken into account in this first approach. Although, the effect of other intermediate species on the enthalpy has been added to the mixture enthalpy.

The flamelet library has been used to simulate a fire in a rock tunnel with and without re-circulation of combustion gases. The simulated temperatures and major species concentrations agree well with measured results.

The chemistry of hot gas layer has been investigated with respect to CO production with the chemical kinetics code CHEMKIN. The different parameters varied are the equivalence ratio, temperature, oxygen, unburned fuel, and incomplete combustion products.

A simple calculation of soot formation in the gas layer has also been made. The results show that in the presence of acetylene in rich mixtures the soot production rate is proportional to acetylene concentration. The soot formation increases rapidly when the temperature is increased to about 900 °C. An increase in the O_2 concentration drastically decreases the soot formation.

Key words: CFD models, flamelet model, under-ventilated fires, chemical kinetics, gas layer, soot formation

SP Sveriges Provnings- och Forskningsinstitut
SP Rapport 1999:03
ISBN91-7848-757-9
ISSN 0284-5172
Borås 1999

SP Swedish National Testing and Research Institute
SP Report 1999:03

Postal address:
P O Box 857, SE-501 15 BORÅS, Sweden
Telephone +46 33 16 50 00
Telefax +46 33 13 55 02
E-mail: info@sp.se
Internet: www.sp.se

Table of contents

	Abstract	**2**
	Table of contents	**3**
	Sammanfattning	**4**
	Nomenclature	**5**
1	**Introduction**	**7**
2	**CFD model SOFIE**	**9**
2.1	Background	9
2.2	Sub-models	9
3	**The laminar flamelet model**	**10**
3.1	Calculated flamelets	11
3.1.1	Vitiated flamelets	12
3.2	Implementation of flamelets into SOFIE	13
3.3	Degree of vitiation	15
4	**CFD simulations**	**16**
4.1	Simulation of fire tests in the Botele tunnel	16
4.2	The scenario	17
5	**Results and comparisons with experiments**	**18**
5.1	No re-circulation	18
5.2	Variable vitiation fraction	21
5.3	Constant vitiation fraction	21
5.4	Comparison with experiments	21
6	**Hot gas layer chemistry**	**25**
6.1	CHEMKIN calculations	26
6.2	Formation of soot precursors	27
6.3	Formation of soot in the hot gas layer	28
6.4	Formation of CO from soot in hot gas layer	29
7	**Discussion and conclusions**	**30**
8	**Acknowledgements**	**32**
9	**References**	**33**
	Appendix A	**35**

Sammanfattning

I detta projekt har beräkning av s.k. flamelets för heptan, propan och metan utförts. Flamelets har beräknats för luft innehållande av olika halter av förbränningsprodukter för att simulera återcirkulation av brandgaser till branden. Beräkningarna har gjorts med s.k. Arclength Continuation Method, vilket innebär att man får effekten and flamtöjning (som sker pga turbulens)in i flamelet data. Beräkningarna baserar sig på ungefär 2000 elementära reaktionsteg, och med ca 100 kemiska ämnen. Som återcirkulerande gaser både varma (1000 K) och kalla (300 K) förbränningsprodukter har betraktats.

Heptanflamelets för olika återcirkulation, färdiga för att använda direkt i SOFIE har skapat ur dessa huvubibliotek. För SOFIE har endast de vanligaste ämnen som ingår i förbränningen,O_2, H_2O, CO, CO_2, N_2 och bränsle tagis med. Inverkan av mellanprodukters entalpi, har inkluderats i det totala blandningsentalpin.

Flamelet biblioteket har testats för simulering av brand i en bergtunnel, med och utan återcirkulation av brandgaser. Koncentrationer av simulerade ämneskoncentrationer stämmer väl med uppmätta resultat.

Kemin i heta gaslagret som uppstår i rumsbränder har också undersökts. Främst faktorer som inverkar på CO produktionen har undersökts. Parametrar som används i beräkningen av: ekvivalenskvoten, temperatur, syrekoncentration, restbränsle, och ofullständiga förbränningsprodukter, har också betraktats.

En enkel beräkning av sotbildning i det heta gaslagret har också gjorts. Resultaten visar att sotproduktion är proportionell mot acetylen koncentration i feta blandningar.Sotproduktionen ökar snabbt då temperaturen närmar sig ca 900 °C men minskar drastiskt då koncentrationen syrgas ökar.

Nomenclature

A_f	Pool area
A_f, A_b	Arrhenius pre-exponential factors in forward and backward rates
C_a	Coagulation rate of soot
C_{min}	Number of carbon atoms in the incipient carbon particle
$C_{\phi i}$	Concentration of species ϕ_i
D	Diffusion coefficient
E_f	Activation energy in forward reaction
E_b	Activation energy in backward reaction
h	Heat transfer coefficient
ΔH_c	Latent heat of combustion
k	Turbulent kinetic energy
k_f	Rate constant of forward chemical reaction
k_b	Rate constant of backward chemical reaction
$\dot{m}$	Mass flow rate of fuel
M_i	Molecular weight of specie i
M_s	Molecular weight of carbon in soot model
N	Number density of soot particles
N	Number or reactions in Appendix A
N_A	Avogadro's number
NS	Total number of species in chemical model
$\dot{q}$	Heat release rate
r_o	Fuel to oxidiser ratio
r_i	Rate constants in soot model
R_f	Forward chemical reaction rate
R_b	Backward chemical reaction rate
R	Universal gas constant
S	Source term in soot model
t	time
T	Temperature
Y_i	Mass fraction of specie i
Y_F	Mass fraction of fuel
Y_s	Mass fraction of soot
β_f, β_b	Temperature exponents in forward and backward reaction rates
γ_f	Third body reaction exponent in forward reaction
γ_b	Third body reaction exponent in backward reaction
ε	Dissipation of turbulent kinetic energy
ϕ	Scalar in flamelet model
ϕ	Equivalence ratio
ρ	Density
ρ_s	Density of soot
κ	Botlzmann constant
ξ	Mixture fraction
ν	Stoichiometric oxidiser-to-fuel ratio
τ	Residence time

σ_m	Reciprocal of mean molecular weight
σ_i	Number of species i
χ	Scalar dissipation rate
ψ	Vitiation fraction
ν_i'	Stoichiometric coefficient of specie i appearing as reactant
ν_i''	Stoichiometric coefficient of specie i appearing as product

1 Introduction

Under-ventilated fires have been previously studied in BRANDFORSK projects reported in references [1-4]. The study reported in [1], describes the method of calculation of the chemistry, a so called laminar flamelet model, and how it can be used in turbulent flames such as fires. In the study presented in [3] laminar flamelets are used in CFD calculations of under-ventilated fires.

Despite the rapid development of modern computer technology, computer time and storage are still the major factors which limit calculations concerning the number of chemical species. Hence, one is generally restricted to the main combustion products and a small number (3-8) of chemical reactions when including chemical information into CFD calculations. This small number of reactions generally gives sufficient detail for most practical fire problems. However, advanced chemical kinetic computer codes exists, which can treat 2000 reaction chemical mechanisms with calculation times not longer than a day. The incorporation of such detailed mechanisms would represent a significant improvement in the ability of CFD modelling to describe the evolution and movement of chemical species in a fire.

To use such large chemical mechanisms in CFD is practically impossible because storage of such a large amount of data for each control volume places such great memory requirements that even modern PCs do not have enough memory. In some specific cases, where one is particularly interested in examining the chemistry more thoroughly, a large chemical scheme could be of interest. An example of this could be to check which species are formed in the hot gas layer in a room fire for a given hot gas layer temperature and composition. Another example could be to calculate the rate of hazardous, chemically stable, substances emitted in a chemical fire. The spread of such substance in flows caused by fires could then be calculated using CFD.

Work in previous projects has been restricted to the calculation of combustion of methane. In this project more complex hydrocarbons, such as heptane, are considered and flamelet calculations are performed using more reactions and species. Further the chemistry of the hot gas layer, in particular with respect to the formation of CO, are examined.

In contrast to zone models which use a few large control volumes, CFD models use a large number of small control volumes to calculate the local values of temperature, velocity, enthalpy, and species concentrations. CFD models numerically solve the full partial differential equation set describing the local conservation of mass, energy, momentum and chemical elements.

As there is no limit to the size and number of control volumes (other than that due to limits in computer capacity), the calculation domain may be divided finely enough to allow a turbulent flow field to be described in terms of a laminar microstructure. Thus, details of the flame structure and chemistry can be calculated. Similarly, the flow pattern and temperature gradient around, e.g., a sprinkler bulb or beam member, can be calculated.

Carbon monoxide is always formed in fires. Even small amounts of CO in the air is dangerous to human beings. Approximately two of three deaths in fires are thought to be due to inhalation of CO. In traditional CFD calculations it is not possible to calculate the concentration of CO in the fire gases, or its propagation with these gases in the volume studied. Using CFD modelling coupled to even a simple chemical mechanism it is possible to obtain a qualitative description of both CO production and distribution in the studied volume. This information represents a major increase in our ability to determine the spread of the deadly products of fires. If a more detailed chemical model, such as the laminar flamelet model applied as a part of this work, is used then quantitative information may be obtained.

The work presented in this report aims at marrying the results of complex laminar flamelet calculations, describing the microscopic chemical behaviour of the species in a fire, to CFD calculations describing gas flow through a well defined volume. Using this combination of techniques one is able to move the regime of fire modelling a step closer to providing us with detailed information concerning the movement of toxic gases in fire compartments.

A short background of the CFD code is given in the next chapter followed by a description of the laminar flamelet model, including details of its use in the CFD calculations. The CFD calculations are described in Chapter 4 with the calculated results presented and compared to experimental results in Chapter 5.

A study of the chemistry in the hot gas layer using the Well-Stirred Reactor (WSR) model is presented in Chapter 6 and a final discussion of all the results and conclusions is presented in Chapter 7.

2 CFD model SOFIE

2.1 Background

CFD models have been used in solving various kinds of fluid mechanical problems for several decades. In fire applications, however, they have only been introduced in the past decade. Thus, most CFD codes have poor facilities, if any, to calculate the events occurring in fires. Approximately 8 years ago, the question of creating a special CFD code specifically for solving fire problems was raised. This has lead to the development of SOFIE (Simulation Of Fires In Enclosures) [6].

SOFIE has been developed at Cranfield University in UK (where further development of the code continues), with sponsorship from the Swedish National Testing and Research Institute (SP) and Lund University in Sweden; the Technical Research Centre of Finland (VTT) in Finland; the Centre Scientifique et Technique du Batiment, CSTB, in France; and the Health and Safety Executive, Fire Research Station (FRS) and the Fire Research and Development, Home Office in England.

Although SOFIE has only been available for a few years, it has been used successfully to simulate fires in several types of enclosures [6-8].

2.2 Sub-models

SOFIE employs most base features needed for computation of fluid dynamics problems and several additional sub-models specifically related to fire and combustion simulations. The base code includes several optional solvers (either steady state or first order implicit transient type) such as Line-by-line Gauss-Seidel, Bilinear/ILU/IC pre-conditioned conjugate gradient and Stones Strongly Implicit Procedure (3D). SOFIE uses general non-orthogonal curvilinear co-ordinates with finite volume discretisation and non-staggered Cartesian velocity components. Pressure smoothing is achieved through momentum interpolation with optional interpolation schemes such as Upwind, Hybrid, PowerLaw, QUICK, SOUP, TVD and QUICKB. Pressure correction algorithms SIMPLE and SIMPLEC can be chosen. The $k - \varepsilon$ turbulence model with buoyancy production modification term is used for calculation of turbulence.

Additional physical models for computing situations occurring in fires include two widely used heat release models: the Eddy break-up [9], modified by Magnussen [10], and the laminar flamelet model [11]. For calculation of the radiation exchange between fluid and solid walls of the enclosure, a discrete transfer model (DTRM) [12] is available. Further, the absorption coefficient models: WSGG (Truelove, Taylor-Foster) and Modak and Leckners's model are available. Soot formation (nucleation, coagulation and surface growth) and oxidation can be modelled using Magnussen (Tesner) model or the Two-Scalar Transport model (flamelet source terms).

3 The laminar flamelet model

The species mass fractions, enthalpy, temperature, soot concentration and any other thermochemical parameter, are quite well known across a laminar flame sheet, and these can be given in terms of a conserved scalar [11], a so called mixture fraction. The mixture fraction states what fraction of the mixture originates from the fuel at a given point in the laminar flame sheet. In other words, there are unique state relationships for all thermochemical parameters in terms of the mixture fraction across a laminar flame.

The laminar flamelet concept can be applied to turbulent diffusion flames (such as fires) by assuming that the turbulent flames consist of microscopic elements, which have the structure of an undisturbed laminar diffusion flame. The relationships are averaged for turbulent diffusion flames using a probability density function (pdf).

By assuming that the chemical reactions occur only in these thin flame sheets (flamelets) and that the chemical time scale is short compared to other time scales (such as diffusion and turbulent transport properties), which is always true for buoyant flames at atmospheric pressure, the statistical uncertainties in a turbulent flow field can be de-coupled from the complex multi-component reaction chemistry. This assumption is accompanied by the fact that the instantaneous species concentrations, temperature and thermochemical parameters are only functions of a conserved scalar [11], i.e

$$\phi = \phi(\xi) \tag{1}$$

where ϕ denotes any scalar variable and ξ, the mixture fraction defined as

$$\xi = \frac{\nu Y_F - Y_{O_2} + Y_{O_2,2}}{\nu Y_{F,1} + Y_{O_2,2}} \tag{2}$$

where ν is a stoichiometric oxidiser-to-fuel ratio, Y_i denotes the mass fraction of species i. The fuel is denoted by index F while O_2 denotes oxygen. The indices 1 and 2 denote initial fuel and initial oxidiser streams, respectively. The stoichiometric mixture fraction ξ_{st} can be expressed

$$\xi_{st} = \left(1 + \frac{\nu'_{O_2} M_{O_2} Y_{F,1}}{\nu'_F M_F Y_{O_2,2}}\right)^{-1} \tag{3}$$

where ν'_{O_2} and ν'_F are the stoichiometric coefficients for oxygen and fuel, respectively, and M_{O_2} and M_F are molecular masses for oxygen and fuel, respectively. Using the expression for oxidiser to fuel ratio r_o equation (3) becomes

$$\xi_{st} = \left(1 + \frac{r_o}{Y_{O_2,2}}\right)^{-1} \tag{4}$$

The flamelet profile is, however, influenced by the local hydrodynamic strain field, which affects the chemical reaction rate. To take strain rate into account the flamelet profiles should be supplemented by information about the local strain field

$$\phi = \phi(\xi, \chi) \tag{5}$$

where χ denotes the scalar dissipation defined as

$$\chi = 2D \frac{\partial \xi}{dx} \frac{\partial \xi}{\partial x} \tag{6}$$

where D is the diffusion coefficient. The scalar dissipation is proportional to the inverse of the strain rate. If one assumes that the turbulent flame is an ensemble of laminar flamelets of well defined structure, the detailed chemistry computation can be separated from the flow field calculation. In this case the modelling can proceed by determining the flamelet state relationships as a function of the conserved scalar and this information can then be stored in library files. Detailed chemical kinetics can then be incorporated into CFD models without an inordinate increase in computer time, as these flamelet relationships can be used again and again during the flow field calculations. Thus, the chemistry does not need to be calculated separately at each node and time step. This method does, however, require a great deal of computer storage space. Further, for practical reasons the flamelet calculations are generally conducted for a finite number of cases and the chemistry is included in the CFD model in a stepwise manner. Thus, discrete pieces of information are available as opposed to a continuous description, and interpolation or approximation must be used when applying the library files. This is described in more detail below.

3.1 Calculated flamelets

In the absence of mixing of reactants (fuel and oxidant) prior to combustion there are substantial inhomogeneities in both mixture and temperature, which will promote the formation of incomplete products of combustion, such as CO. Re-circulation of combustion products reduces the rate of chemical reactions and combustion efficiency which also increase the amount of incomplete combustion products in fire gases.

The composition and temperature of the air entrained into the fire may vary considerably during a room fire. At the very beginning of the fire the oxidant stream is almost pure air at room temperature. Depending on the shape and size of the room and fire, and the fuel type and ventilation, the oxidant stream may be vitiated and its temperature may rise, as the fire grows. To accommodate these different situations, the flamelets are calculated for several degrees of vitiation, and at a variety of temperatures. The calculated flamelets are stored in a data base, the so called flamelet library. The composition and temperature of oxidant stream are checked during the flow field calculations and the most suitable flamelet state relationships are extracted from the data base for use in calculations for the next time steps.

3.1.1 Vitiated flamelets

In this study the flamelet calculations are performed in several oxidiser environments: in pure air at 300 K, air mixed with combustion products at 300 K, and air mixed with combustion products at 1000 K. Thus, the temperature of the oxidiser stream was dependent on the vitiation due to the mixing of hot combustion gases with pure air. The temperature of the oxidiser stream as a function of the vitiation fraction is summarised in Table 1. Equal and constant heat capacities are assumed for the combustion products and air. The combustion products in the oxidiser stream are assumed to consist only of H_2O and CO_2 in proportions corresponding to stoichiometric combustion of the fuel. All flamelet calculations were performed at 1 bar pressure, the radiation was omitted and, scalar dissipation rates from $\chi = 0.01\ s^{-1}$ up to extinction value of χ were used.

Table 1: Oxidiser stream temperatures for various values of the vitiation fraction used in the flamelet calculations.

Vitiation fraction	Temperature of oxidiser stream [K]
0	300
0.2	440
0.4	580
0.6	720
0.8	860

The flamelet calculations carried out in this study used the so called Arclength Continuation Method [13], which solves a set of differential equation, including the inverse of scalar dissipation rate as a variable.

In reality the rates of chemical reactions are reduced when the reactions occur in vitiated air, due to the reduced oxygen mass fraction in the oxidant stream. In this study, however, it is assumed that the chemistry is still sufficiently fast, such that the laminar flamelet concept can be applied, even at as high vitiation fraction as 0.80. Thus, the degree of vitiation influences the flamelet profiles, but generally the profiles are of the same shape. The stoichiometric point is shifted to lower values of mixture fraction because the oxidiser stream is now defined as the mixture of pure air and combustion products. The stoichiometric mixture fraction in vitiated environment can be calculated using Eqn (4) by replacingthe pure air stream, $Y_{O_2,2}$, by the vitiated air stream $Y_{O_{22},2}(\psi)$, as below:

$$\xi_{st} = \left(1 + \frac{r_o}{Y_{O_2,2}(\psi)}\right)^{-1} \tag{7}$$

where ψ is a vitiation fraction. The variation of the stoichiometric mixture fraction in a vitiated environment for methane, propane and heptane is shown in Table 2.

Table 2: Variation of stoichiometric mixture fraction with the degree of vitiation for methane, propane and heptane.

Vitiation fraction [ψ]	0	0.2	0.4	0.6	0.8
Oxygen mass fraction	0.232	0.186	0.140	0.093	0.046
Stoichiometric mixture fractionMethane	0.055	0.045	0.034	0.023	0.0115
Propane	0.060	0.049	0.037	0.025	0.0125
Heptane	0.068	0.050	0.038	0.026	0.0129

The largest difference between vitiated and non-vitiated flamelets is that the peak values of mass fractions of important radicals that control the combustion are considerably lower for vitiated flamelets. The larger the degree of vitiation, the lower the peak value. Other important differences are that the peak values for the temperatures and CO concentrations are lower and the CO_2 and H_2O concentrations higher. Note that the reduction of peak values of CO, and increase of CO_2 and H_2O values does not mean that more CO_2 and H_2O, and less CO, are produced in combustion in the vitiated atmosphere. Due to vitiation the oxidiser stream already contains CO_2 and H_2O before combustion. Hence, in the vitiated flamelet, profiles represent the sum of calculated and initial concentrations of these gases. The explanation to lower CO concentrations is that the values represent the fraction of the total mass of the mixture. Actually the production of CO increases in proportion to the amount of fuel combusted with increased vitiation. For methane this increase is about 35 % when the vitiation fraction is increased from 0 to 0.60 using hot combustion products. For cold gas vitiation the increase of CO per mass unit of methane is about 150 % [1-2]. Profiles of methane flamelets for different degrees of vitiation are shown in reference [1].

3.2 Implementation of flamelets into SOFIE

The current version of SOFIE uses calculated lookup tables for flamelet properties during the flow field calculation. Such tables can be created by SOFIE from tables of flamelets. In the tabular flamelets all the species, temperature, enthalpy, density and other important thermochemical parameters are represented as a function of mixture fraction. When the radiation is included the different columns for radiation are included in the flamelet table. The structure of the flamelet library for vitiated heptane flamelets is shown in Figure 1. The structure of vitiated flamelet libraries for other fuels is similar.

The lookup tables for all scalars are created at the SOFIE command prompt (either interactively or using a script file). When calculating the lookup tables SOFIE also creates the mixture fraction variance using the beta function.

When including fire gas re-circulation one additional dimension is included in flamelet profiles. The lookup tables are then supplemented by information about the vitiation fraction. If vitiation up to 80% is taken into consideration and the vitiation fraction is incremented by 0.2 then the lookup tables for each variable becomes 5 times larger than without considering vitiation.

When the effect of scalar dissipation is taken into account a further dimension is added and thus the lookup tables will become even larger.

All flamelet calculations used in this study have been conducted as a part of a project conducted at Lund Technical University by Dr Fabian Mauss.

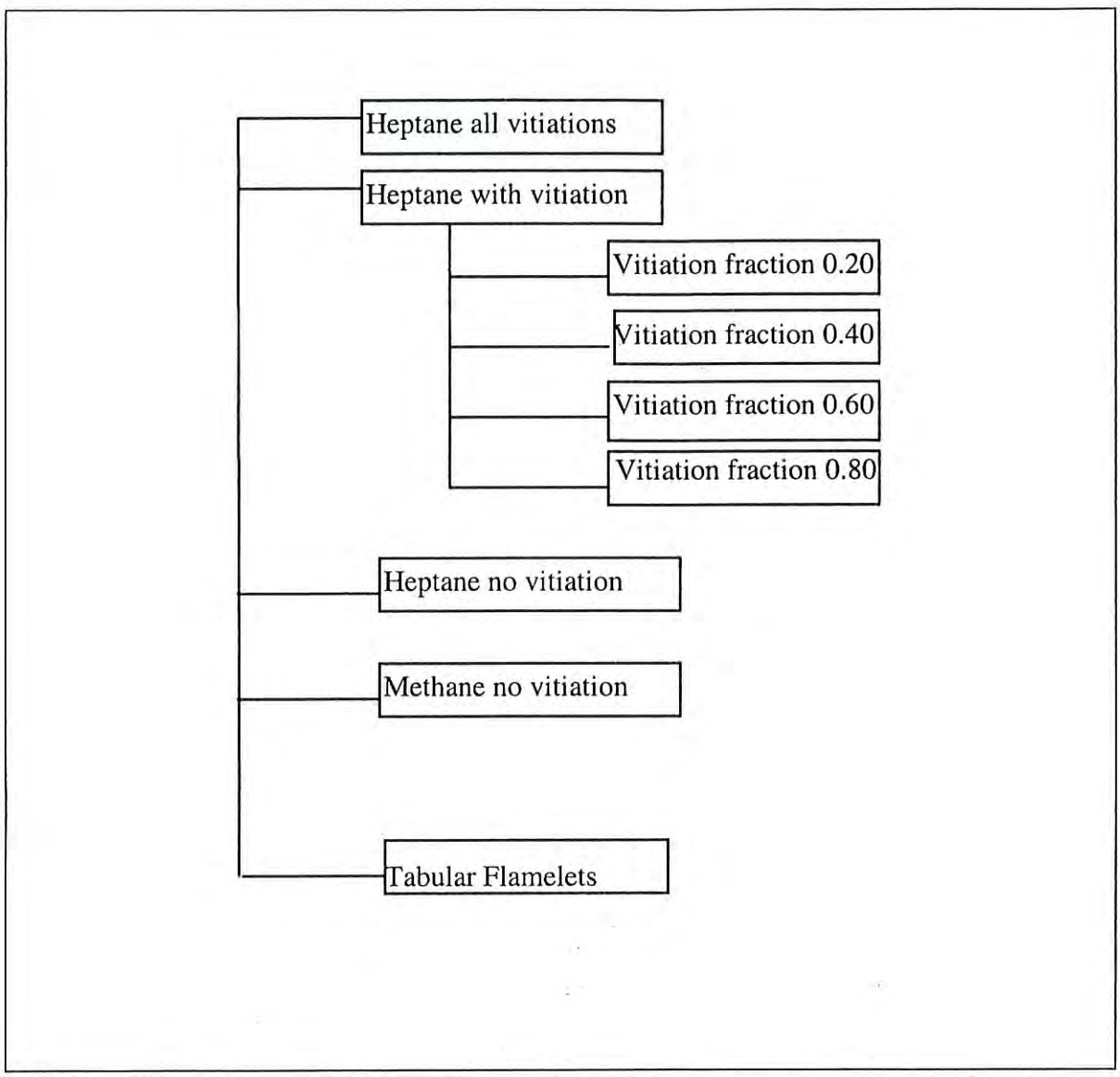

Figure 1: Flamelet library structure used in the current version of SOFIE. The flamelet calculations for heptane are based on the chemical scheme of 2000 elementary reaction steps involving more than 100 species. Separate sets of flamelets for vitiation fractions of 0, 0.20, 0.40, 0.60 and 0.80 are included.

3.3 Degree of vitiation

The use of vitiated flamelets does not differ from the use of non-vitiated flamelets. During the flow field calculation the information about mixture fraction and its variance in each control volume, is stored in computer memory together with all other parameters such as species concentrations, temperature and enthalpy. The simplest check of the vitiation fraction, ψ, in a specific control volume is to compare the oxygen mass fraction at that location with the value in the fresh air,

$$\psi = 1 - \frac{Y_{O_2}}{Y_{O_2,\infty}} \tag{8}$$

where $Y_{O_2,\infty}$ is the oxygen mass fraction in fresh air. In this study this check is made only in the entrainment region. The flamelets closest to this vitiation fraction are then used until an update of the vitiation fraction at this location is made.

4 CFD simulations

4.1 Simulation of fire tests in the Botele tunnel

A large number of fire tests have been carried out in a 100 m long blasted rock tunnel with a cross-sectional area of 9 m^2 (3 m wide and 3 m high tunnel) [14]. The tunnel had a 12.3 m high shaft for fire gas ventilation (natural ventilation) at one end and was open at the other end. To vary the degree of ventilation a steel wall was placed in the tunnel 26.6 m from the centre of the shaft. The steel wall was sealed, except for an opening of diameter 0.64 m in the centre of the tunnel, 1.2 m above the ground. A 6 m long pipe was connected to the opening, through which the fresh air was lead into the tunnel. The size of the inlet opening to the pipe was variable to enable the adjustment of the air inlet to the tunnel. A schematic representation of the tunnel is shown in Figure 2 [14]. During the experiments the wall was found to leak and thus the effective size of the inlet opening was larger than measured at the pipe.

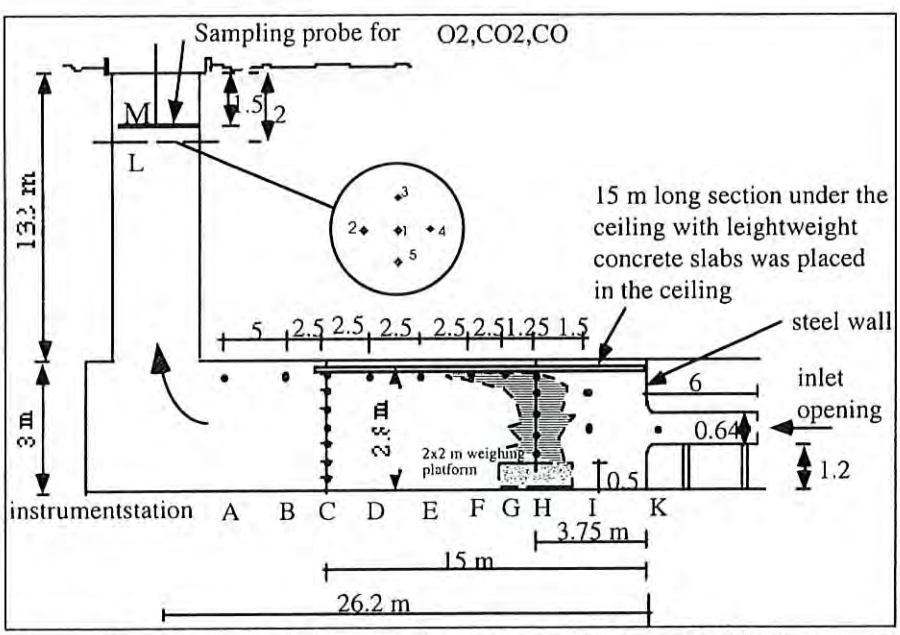

Figure 2: A sketch of the tunnel used in the tests [14]. The instrument locations are denoted by letters A through M.

In the simulations some simplifications were made: the entrance pipe was omitted and the fresh air flow equal to the flow through the pipe was modelled as the inflow boundary at the inner end of the pipe. The cross section of the simulated vertical shaft was rectangular rather than circular. The concrete plate at the ceiling, above the fire region, was also omitted. Initial simulations indicated that the flow measured in the experiments underestimated the air flow into the tunnel by a factor 5. During the fire experiments the pressure on the fire side of the wall blocking the tunnel was below atmospheric pressure. It is assumed that under these conditions the wall leaked air from the blocked part of the tunnel. This assumption is confirmed by the observation during the experiments that the wall was close to collapse. Thus, the inflow of the air and size of the inflow aperture has been adjusted to what is believed to be a more realistic estimate of the true inflow conditions

4.2 The scenario

Some minor simplifications to the tunnel geometry shown in Figure 2 were made to facilitate the CFD calculations. The tunnel was modelled having a rectangular cross-section (3×3 m^2) as was the exhaust shaft (1.33×1.33 m^2). Similarly, the inflow was modelled to have rectangular cross-section with area equal to the real circular cross-section including a suitable adjustments of the inflow side as described above. The shaft in the CFD model was placed in the tunnel centreline rather than off centre. The steel plate and pipe were omitted. All wall boundaries were modelled as inactive blockages. Isothermal boundary conditions were used with a convective heat transfer coefficient of $h = 25.0$ J/ m^{2}K at all inner wall boundaries.

In the tests several fuels and ventilation conditions were considered. One scenario was simulated using three options, to study the performance of the laminar flamelet model with fire gas re-circulation. In this scenario a 0.65 x 0.65 m^2 heptane pool was simulated. The three different options were:

- a flamelet model with no re-circulation of combustion products in air stream, i.e. vitiation fraction $\psi = 0.0$
- a variable vitiation fraction using combustion products in the air stream equal to those calculated by SOFIE for the entrainment region
- a constant vitiation fraction, $\psi = 0.40$.

The two cases with re-circulation were run using hot combustion products in the air stream. The temperature of the air stream was set according to Table 1.

The flamelet profiles used in the study were based on calculations using about 2000 elementary reaction steps involving about 100 species. Only the main species CO, CO_2, H_2O, and O_2 were included in SOFIE, and only CO_2, H_2O and N_2 were recirculated. This can be displayed in three dimensional plots throughout the whole calculation domain, in the same way as can the temperature and flow velocities.

5 Results and comparisons with experiments

All the CFD simulations were carried out using exactly the same computational mesh, heat release rate and boundary conditions. Due to the differences in the convergence behaviour of the calculations, based on the degree of vitiation, slightly different relaxation parameters were used to obtain the best solution for each scenario.

A time step of one second was found suitable in all cases. The scenario with no recirculation (i. e: $\psi = 0$) was run up to 4 minutes. In the case with variable vitiation the first two minutes were used without recirculation, i. e. vitiated gases were included in the oxidant stream only after the first two minutes. This was chosen due to the somewhat contrived way recycled fire gases are included in calculation. In the initial calculation the recycled fire gases are included as a fraction of the oxidant stream and only H_2O, CO_2 and unreacted N_2 are recycled. If vitiation were included from $t = 0$, then an unrealistic amount of CO_2 would be included in the oxidant stream (with a corresponding depletion in the concentration of O_2) before the fire has had time to produce CO_2. After $t = 2$ min a vitiation of $\psi = 0.2$ was used.

Finally a scenario was run with $\psi = 0.4$ from $t = 0$ to 2 minutes. The oxidant flow in this case is assumed to contain 40 % combustion products. Thus the combustion efficiency is initially very low. Further recirculation of combustion products into the flame region reduces the ability of the system to sustain combustion, i. e. the recycled fire gases effectively extinguish the fire.

5.1 No re-circulation

In this scenario non-vitiated heptane flamelets were used.

The mass flow rate of fuel was adjusted to the same value as in the experiments, i. e 0.08 kg/m^{2}s across the pool area of 0.4445 m^2 (0.65 x 0.65 m^2), corresponding 0.0338kg/s of total fuel mass flow rate. This fuel flow rate was used during the whole simulation time except for first two minutes when the mass flow was reduced by 30 % to take the lower fuel vaporisation rate in the warming-up phase into account. Using these boundary conditions SOFIE then calculates the rate of heat release. The maximum heat release rate can be calculated using

$$\dot{q} = \Delta H_c \dot{m} \cdot A_f \qquad (9)$$

where ΔH_c is the latent heat of combustion of the fuel, $\dot{m}$ is the mass flow rate of fuel and A_f is the pool area. Using equation (9) and $\Delta H_c = 4.67 \times 10^7$ J/kg the maximum heat release rate (based on the data cited above) is 1.58 MW. SOFIE takes the oxygen content in the air into the calculation and reduces the heat release rate if the oxygen concentration is sufficiently reduced. Unburned fuel is left in the downstream flow from the fire source.

The experimental measurements of the inflow of air fluctuated between 0.2 and 0.5 kg/s with an average value of 0.4 kg/s. This value was used in the initial calculations. The concentration of CO_2 increased rapidly in these calculations to a level approximately 3-4 times that measured in the tunnel. Similarly the O_2 concentration decreased to such an extent that the fire became self-extinguishing which caused severe convergence difficulties. After further simulations and comparisons between inflow and exhaust it was determined that the experimental measurements of inflow of the air have severely underestimated the true inflow. The true value is estimated to be approximately 2.5 kg/s and

is thought to be due to leakage of air into the tunnel through cracks in the barrier constructed to shut off the end of the tunnel. This conclusion is supported by the observations during the experiments that this barrier was close to collapse.

As a first step the air inflow was about 1 kg/s. The combustion efficiency was increased, but there were still large discrepancies in species concentrations and velocities, which indicates that the air inflow into the tunnel has not been corrected sufficiently. Thus, from $t = 3$ min the air flow into tunnel was increased to 1.3 kg/s in order to increase the gas velocity at the ceiling to about the same values as those measured. The results at $t = 4$ min showed much better agreement with the measured result for the most measuring locations.

The true flow into the tunnel is a function of the pressure in the tunnel. As the fire increases in size the pressure on the fire side of the barrier decreases and the inflow of air increases. Thus, this stepwise increase in air flow mimics experimental conditions realistically.

The results for $t = 4$ min for these calculations are shown in Figures 3, 4 and 5 for O_2, CO_2 and CO, repectively.

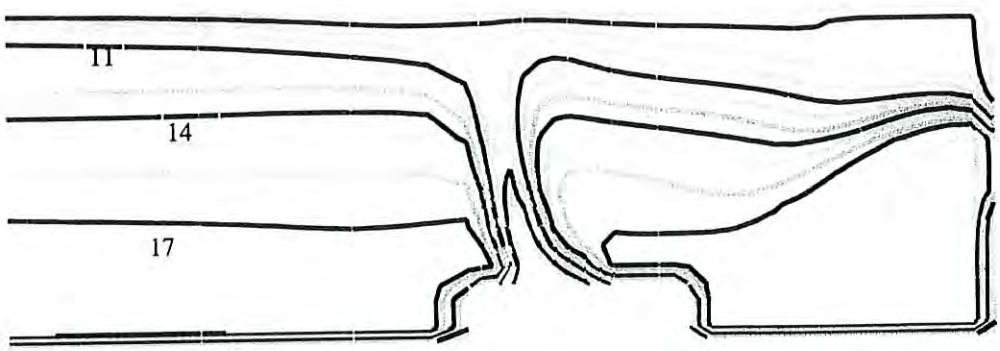

Figure 3: O_2 concentration field at near fire region. Scenario with no vitiation, time 4 min after the ignition. The numbers in the figure states the concentration of O_2 in % by volume.

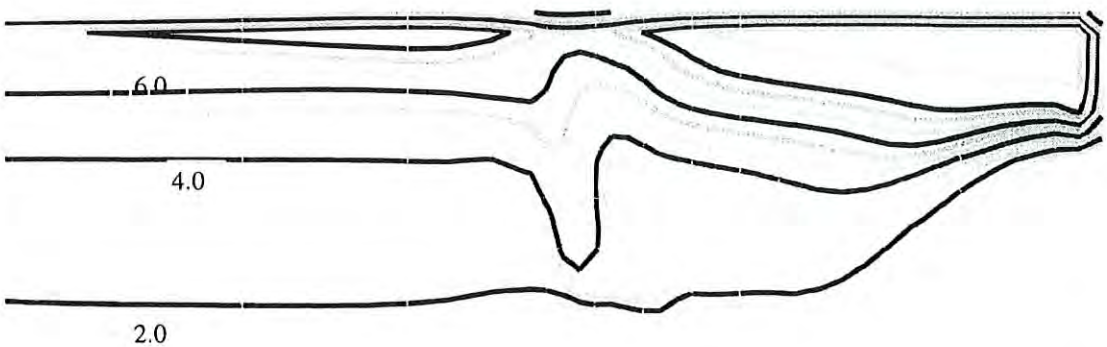

Figure 4: CO_2 concentration field at near fire region. Scenario with no vitiation, time 4 min after the ignition. The numbers in the figure states the concentration of CO_2 in % by volume.

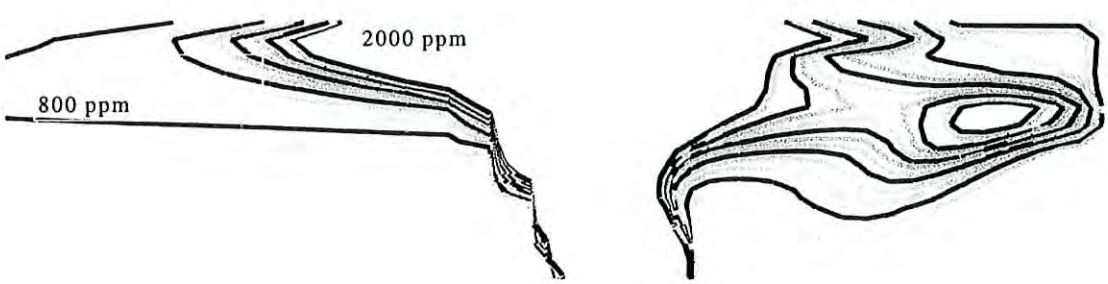

Figure 5: CO concentration field at near fire region. Scenario with no vitiation, time 4 min after the ignition. The thick line are increments of 300 ppm.

5.2 Variable vitiation fraction

The scenario with no vitiation, presented in Section 4.1, while providing a good description of the fire development in the early stages, does not properly describe the experimental evolution as the concentration of fire products builds up.

To include the effect of vitiation on the chemistry of the fire, the concentration of the main products (CO, CO_2, HO_2) and O_2 were checked for a few control volumes in the entrainment region of the fire. The vitiation fraction was calculated using Equation 8. Hot combustion products were assumed to re-circulate to the fire. At the time two minutes after the ignition the mean vitiation fraction at the entrainment region was increased to the vicinity of 0.20 and the corresponding set of vitiated flamelets were brought in to the calculations at this time.

A comparison between these results, those presented in Section 5.1 and experimental results is given in Section 5.4.

5.3 Constant vitiation fraction

In order to investigate the propensity of any given fire to spread to an adjacent compartment it is necessary to study the ability of the new compartment to initiate or sustain combustion. In this case the oxidant stream contains fire gases from $t = 0$ min. This scenario has been studied with a constant vitiation of 0.4 throughout the whole simulation.

This vitiation fraction appeared to be unrealistic in this tunnel as the fire rapidly cooled and self-extinguished. Thus, the simulation was stopped after two minutes. Within this period the concentrations of CO_2 became unrealistically high, and O_2 concentration fell so low that combustion ceased.

Thus we concluded that the model was able to describe a scenario with vitiated oxidant stream from t=0 min, but that this specific application was identified as unrealistic for sustained combustion.

5.4 Comparison with experiments

The calculated gas temperatures and velocities and the major species concentrations have been compared with measured result at most measurement stations. A comparison has been made for scenarios with no re-circulation and variable re-circulation at four min after the ignition. In the case of constant vitiation the results are only discussed relative to the scenario with no re-circulation. This comparison is shown in Tables 3, 4, 5 and 6. Table 3 shows the comparison of simulated gas temperatures with measured values at tunnel centreline, 15 cm below the ceiling at different locations A-H, as defined in Figure 2 with the fire located at H.

The high value of the temperature at point G in the simulated non-vitiated case is due to the tilt of the fire plume so that the fire plume near the ceiling hits the instrument location. It is always difficult to compare results close to the fire, as the flames are not steady. At one point in time the thermocouple may be overwhelmed by flames and not at another. The experimental temperatures are determined by smoothing of the experimental curves for each of the measurement points and evaluating the temperature at the desired time. The calculated temperatures represent the temperature average of the appropriate cell. Hence, the temperature at a given location near the fire may vary strongly in time. Further, a small difference in the tilt of the flame may cause a large difference in the mean

temperature at any given location. A few cm from this point the simulated temperature is near the measured value. It should be noted that both the simulated models produce the same qualitative behaviour close to the fire with a temperature maximum at G.

Table 3: Comparison of simulated temperatures in °C with measured data 15 cm below the ceiling in different locations A-H at tunnel centreline, 4 min after the ignition. For definition of the locations, see Figure 2.

Location	A	B	C	D	E	F	G	H
Measured	230	264	322	341	409	518	791	973
Simulated,non vit	148	207	255	331	453	656	1004	982
Simulated, var.vit	192	248	335	350	446	582	734	587

The temperature 15 cm below the ceiling is also shown graphically as a function of distance from fire in Figure 6. Beyond 5 m from fire the simulated gas temperatures are quite well correlated with measured values. The best agreement is shown for the case with variable vitiation, the simulated temperatures are essentially equivalent to the measured values in this region. In the non-vitiated case the temperatures are higher (10-20 %) near fire region and lower (20-30 %) at distances more than 8 m from fire.

A good agreement between simulated and measured result at eccentric located points 15 cm below the ceiling has also been noted. This is illustrated in Table 5.

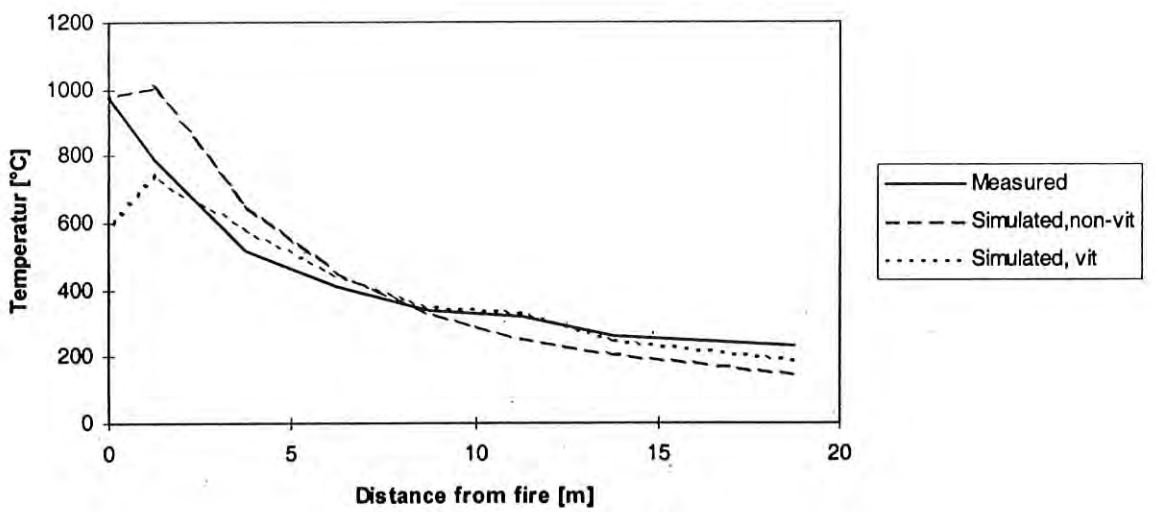

Figure 6: Comparison of simulated gas temperatures 15 cm below ceiling at tunnel centreline as a function of distance from fire.

Due to the decreasing combustion efficiency with increasing vitiation the temperature in the gas layer near the fire region, is reduced, as it can be seen in Table 3. However, at lower levels the simulated temperatures are considerably higher (see Table 4). The reason for this is that in the vitiated flamelets the oxidant steam is assumed to contain hot combustion products, which increased the initial temperature of the oxidant stream. In this case 20% of fire gases (CO_2, H_2O and unburned N_2) at the temperature 1000 K giving the oxidant stream a temperature rise of 140 K (see Table 1).

Table 4: Comparison of simulated temperatures (°C) with measured data at various heights at the tunnel centre line at location C, 4 min after the ignition.

Distance from ceiling (m)	0.15	0.8	1.2	1.8	2.4
Measured	324	195	151	114	83
Simulated, non vit	255	289	270	203	156
Simulated, var. vit	335	311	298	252	220

Table 5: Comparison of simulated temperatures with measured data 15 cm below the ceiling at various distances from the tunnel centre line at location C, 4 min after the ignition.

Distancefrom centre line (m)	0.25	0.50	1.0	1.3
Measured	332	321	259 295*	231
Simulated, non vit	254	250	230	190

*The first value represents a measurement to the left of the centreline while the second value represents a similar measurement to the right of the centreline. In the simulation the average is used as only half of the tunnel is simulated due to symmetry.

The simulated concentrations of CO, CO_2 and O_2 close to the ceiling agree quite well with the measured results. The concentration of CO near the floor, in the simulations and measurements is however, quite discrepant. This is summarised in Table 6.

The simulations yield somewhat higher CO_2 concentrations and lower O_2 concentrations. The CO_2 concentration does not increase noticeably when vitiation is taken into account. However, at the lowest level (1.8 below ceiling) the CO_2 concentration rises from 2.5 to 3.6 when the vitiation is increased from 0 to 20 %.

In the vitiated case the lower value of the simulated CO concentration is partially due to the fact that the previously produced CO is not assumed to recycle to fire (as CO_2 and H_2O are) and the lower combustion rate reduces the rate of CO formation (even though CO production is increased per amount fuel consumed). Assuming CO/CO_2 ratio in recycled gas is to be the same as calculated in gas layer for the non-vitiated case, 20 % vitiation would yield 144 ppm addition of CO at height 1.8 m below the ceiling. This added to 79 ppm calculated in the non vitiated case would yield 223 ppm. An uncertainty arises concerning the amount of ventilated CO at that level. A good guess is that a real value should be somewhere between 223 and 144 ppm CO if re-circulation of CO had been taken into account in flamelet calculations. This is considerably nearer the measured value at that height. All species concentrations are represented in relative concentrations. Thus, the calculated values shown in Table 6 are the sum of recycled and currently produced CO_2 minus ventilated CO_2. This is a definite shortcoming of the method of recycling the fire cases. With only minor modification one could remedy this situation. Inclusion of CO in the recycled fire cases would immediately improve this situation. As CO is an important fire gas from a toxicological point of view such a modification would make the model far more useful.

Table 6: Comparison of the concentrations of CO, CO_2 and O_2 between measured and simulated data at different heights in location C, 4 min after the ignition.

Species	CO (ppm)			CO_2 (vol %)			O_2 (vol %)		
Distance from ceiling [m]	0.15	0.8	1.8	0.15	0.8	1.8	0.15	0.8	1.8
Measured	420	342	249	5.5	3.0	2.5	13.0	16.4	17.4
Simulated, non vit	382	288	79	6.6	5.4	2.5	11.8	14.1	16.7
Simulated, vit	384	292	55	6.7	4.5	3.6	9.6	12.3	15.4

6 Hot gas layer chemistry

The flamelet model as applied in Chapters 4 and 5 is sufficient to describe the chemistry in large parts of the modelled volume. One shortcoming of the model, however, is the fact that chemical reactions are seen to be instantaneous. This approximation is not always sufficient in the hot gas layer. An alternative approach is to treat the hot gases as a well stirred reactor (WSR) with a well defined boundary to the cold gases.

In the WSR model the reactants and products are assumed to be well mixed at the molecular level. Thus, at all points inside the reactor the same physical conditions prevail, i.e the species concentrations are calculated for the reactor as a whole. In the calculations presented in this study the effect of the residence time, τ, and availability of oxygen expressed as the global equivalence ratio, ϕ, on the product distribution, are investigated. Reactants are fed into the reactor via an inlet. These are allowed to react inside the reactor for a given amount time, the so called residence time, τ. The products are then released through the reactor outlet.

The chemical composition of the hot gas layer in room fires depends on many parameters, such as fuel type, ventilation rate and fire size. Especially during under-ventilated, or fuel-rich, conditions the combustion is far from complete which generates CO and other incomplete combustion products. Such products are highly toxic and may cause a fire gas explosion which in turn assists the rapid development of the fire to flashover. In light of the importance of the production of such species a thorough understanding of the processes taking place in the hot gas layer is imperative.

In this application of the WSR model the temperature in the hot gas layer is assumed to be 800 °C, which represents an average temperature in post-flashover fire gases. Due to restriction of the oxygen supply, most well developed fires become oxygen controlled and attain a characteristic behaviour defined by the oxygen supply. This characteristic makes the WSR model particularly applicable to enclosure fires.

To examine the chemistry in the hot gas layer a chemical kinetics code, CHEMKIN [15], including the WSR concept, has been used. The inlet flow in this particular application of the WSR model is essentially from the fire. The outlet concentration corresponds the gas concentration in the hot layer. This depends on the length of a residence time, i. e. the time the reactants are assumed to reside at the hot layer temperatures.

In this study most interest is focused on the production and destruction of CO in the gas layer. The gas composition that prevails in the flow field at a given location in the gas layer, is examined. The length of residence time is chosen with respect to size (i.e. length in the mean flow direction) and gas velocity in that part of the gas layer.

The procedure for this investigation is the following:

A. Feed the combustion products into the WSR in accordance with the measurements in the room fire tests

B. Vary the equivalence ratio, ϕ, and observe the variation of temperature and species concentration, especially, O_2 and CO

C. Vary the input temperature (and possibly the start temperature of gas inside the reactor) and observe the effect on the CO concentration.

D. Vary the O_2 concentration and observe the temperature and CO concentration for given ϕ in the gas layer (In this way the effect of entrainment of O_2 across the layer interface is examined.)

E. Vary ϕ by changing the concentration of unreacted fuel and/or the products of incomplete combustion.

6.1 CHEMKIN calculations

Several calculations using CHEMKIN with the well stirred reactor concept were performed. It was found that fuel rich mixtures equivalence ratios up to $\phi = 3.0$ are most important with respect to CO formation . Therefore, chemical kinetics calculations were focused to ϕ - values between 1.0 and 3.0 with very few calculations made for lean mixtures $\phi < 1.0$. The calculation procedure for each run was the following:

1) The initial gas composition in the reactor for the given equivalence ratio was set the same as in calculated flamelets for that equivalence ratio.

2) The composition of the inflow gas to the reactor was initially exactly the same as the start composition in the reactor, and the composition was varied linearly as a function of time. When, for example, the effect of air entrainment in to the gas layer through the layer interface was examined the oxygen concentration in the inflow was varied from the start value to higher concentrations. Similarly, the effect of unburned fuel in the gas layer was simulated by varying the fuel concentration in the reactor inlet stream as a function of time.

3) The initial temperature of the gas in the reactor and in the inlet stream was set to 800 K. A constant wall temperature of 500 K was used to take into account the convective heat transfer from the hotter gas layer to the wall. The radiation from the fire gases was also calculated using the Modak's model [16,17] which calculates the spectral distribution of radiation from CO_2, H_2O and soot particles. In this study the soot radiation was omitted.

4) The residence time of of the gases in the WSR was varied between 2 s and 10 s. The longer residence time was needed to take slow chemical reactions into account.

5) A chemical model consisting of 146 elementary reaction steps and 38 species was used. During the residence time chosen, the gas mixture was allowed to react in the reactor. The reactor outlet stream represented the calculated composition of the gas layer and gases which were ventilated out through the openings. The chemical reaction mechanism is given in Appendix A

The initial composition of fire gases in the reactor and inlet stream was assumed to contain the following species: CH_4, O_2, H_2O, CO_2, N_2, CO, H_2 and C_2H_2. The concentration of these species, which depends on the appropriate equivalence ratio used in the simulations, was taken from the flamelet state relationships (which are used in SOFIE for calculation of the flow field in this study). Components with concentrations below 1 % were omitted. For example, for $\phi = 2.0$ the gas composition shown in Table 7, was set in the input stream and as the initial gas in the reactor.

Table 7. The initial chemical composition of fire gas for $\phi = 2.0$, in the WSR and inlet stream.

SPECIES	VOLUME FRACTION
CH_4	0.044
O_2	0.05
H_2O	0.101
CO_2	0.0381
N_2	0.5398
CO	0.136
H_2	0.116
C_2H_2	0.0147

To avoid including a detailed chemical kinetics reaction mechanism for the destruction of heptane the unburned fuel in the inlet stream was given such that the fraction of C_2H_6, C_2H_5, C_2H_4, C_2H_2 and CH_4, gave a C/H ratio that was the same as for heptane. This approximation is reasonable, since the bond energy (approximately the heat of formation) of a mass unit of heptane is about the same as the equivalent mass unit for the fractions used.

Result show that the gas layer is ignited when its temperature reaches about 800 K, if the mixture is combustible, i. e. sufficient oxygen, fuel or incomplete products of combustion. The combustible concentration of these components is largely interdependent. For example for mixtures containing very little unburned fuel, about 1 %, but quite large amount of incompleted combustion products, $\phi =$ 2.0, ignition occurs when O_2 concentration is about 3.2 %. Increasing the amount of unburned fuel lowers the level of oxygen concentration available for ignition of the gas layer.

6.2 Formation of soot precursors

When fire gases penetrate the interface between hot and cold layers the chemical chain propagation reactions are quenched due to cooling and lack of oxygen. This results in a flow of incomplete combustion products into the hot gas layer. Some of these products react further in the gas layer depending on the physical conditions which prevail there, such as temperature, concentration of unburned fuel and oxygen, fuel type, etc. The chemistry of these incomplete combustion products is much slower than the chemistry in the flaming region. Thus, the residence time, i.e., flow time of gases through the gas layer influences the species formation in the gas layer. This implies that the formation of certain species is also dependent on the room size and ventilation rate.

The higher the equivalence ratio the higher the formation of C_2H_2, which is assumed to be a major soot precursor. The C_2H_2 formation depends on the temperature and on the type of species in the gas stream into the hot gas layer, i.e. whether it is mainly composed unburned fuel or complete combustion products. In low oxygen mixtures the amount of C_2H_2 formed increases with increasing concentration of unburned fuel.

6.3 Formation of soot in the hot gas layer

Soot formation and (and destruction) is a complicated process. The following steps are usually associated with the formation of soot:

- particle inception, nucleation
- surface growth
- coagulation
- oxidation
- agglomeration

The formation of soot will occur in the hot gas layer as there are large amounts of the soot precursor, C_2H_2, in the gas layer. To examine the production of soot in the hot gas layer the Lindstedt model [18-20] was used. The Lindstedt model solves the transport equations for soot mass fraction and soot particle number density. For laminar flames the source terms are calculated using:

$$\rho S(Y_s) = r_1 M_s + r_2 \rho^{1/2} M_s^{2/3} Y_s^{1/3} N^{1/6} - r_3 \rho M_s^{1/3} Y_s^{2/3} N^{1/3} \tag{10}$$

and

$$\rho S(N) = r_4 - r_5 \rho^2 M_s^{-1/6} Y_s^{1/6} N^{11/6} \tag{11}$$

where the three terms on the right hand side of soot mass source term equation (10) represent the nucleation, surface growth and oxidation, respectively, and the two terms in the right hand side of the number density source term equation (11) represent the nucleation and coagulation, respectively. The individual reaction rates r_1 through r_5 are given by

$$r_1 = 1.0 \times 10^4 e^{(-21100/T)} [C_2H_2] \tag{12}$$

$$r_2 = 1.2 \times 10^2 \left\{ \pi \left(\frac{6M_s}{\pi \rho_s} \right)^{2/3} \right\}^{1/2} e^{(-12100/T)} [C_2H_2] \tag{13}$$

$$r_3 = 715 T^{1/2} e^{(-19680/T)} \pi \left(\frac{6M_s}{\pi \rho_s} \right)^{2/3} [O_2] \tag{14}$$

$$r_4 = 2.0 N_A r_1 / C_{\min} \tag{15}$$

$$r_5 = 2.0 C_a \left(\frac{6M_s}{\pi \rho_s} \right)^{1/6} \left(\frac{6\kappa T}{\rho_s} \right)^{1/2} \tag{16}$$

where M_s is molecular weight of carbon (12 g/mole), ρ_s the density of carbon (1800 kg/m^3), N_A the Avogadro's number, C_{min} denotes the number of carbon atoms in a soot particle (100), κ the Boltzmann constant and C_a the coagulation rate of soot (9.0). The above equations are valid for laminar flames. For the gas layer the problem is more complicated, but let us assume that the trends, concerning the temperature and C_2H_2 and O_2 concentration, are similar for the gas layer. These calculations can therefore give a reasonable picture of soot development there.

According to this model soot formation increases rapidly, for rich mixtures, when the temperature is increased to 900 °C . The soot production is proportional to the C_2H_2 concentration in the hot gas layer. Given a sufficiently high temperature, the soot is oxidised if oxygen is added to the mixture. The most drastic reduction of the soot formation rate occurs for temperatures higher than 1100 °C when the O_2 concentration is increased to approximately 5 % by volume. At temperatures below 1000 °C soot production rate is not greatly influenced by the concentration of O_2. This is due to the highly stable nature of the soot particles.

6.4 Formation of CO from soot in hot gas layer

The presence of soot and CO_2 at high temperatures is assumed to lead to the generation of CO [21]. The above calculations show that large amounts of soot are formed in rich mixtures and that high concentrations of CO_2 are present at same time in the hot gas layer. According to the assumption outlined in reference [21] and the simplified model applied in this study large amounts of CO may be generated in the hot gas layer. In order to determine more precise levels of the CO concentration a more detailed soot formation, oxidation and further CO production simulation together with laboratory tests should be made.

The calculation of the soot formation and oxidation alone would require a much larger chemical reaction mechanism than the one used to calculate the chemistry of the hot gas layer in this study. Further, an additional chemical reaction mechanism would be needed to determine the formation of CO from soot and CO_2. This work would provide insight into the relationship between the production of smoke in a fire and the toxicity of the smoke. This information is important in terms of the ability of people caught in a fire to exit the compartment. Due to the constraints of this project this topic is suggested as future wor

7 Discussion and conclusions

There are quite few well documented experiments of vitiated fires, suitable for the validation of CFD models, available today. Further, to obtain the best possible comparison between measurements and calculations concerning the chemical species compositions, it is necessary to use the same fuel. To test CFD models for the calculation of heptane combustion in vitiated conditions, a fire tests in a blasted rock tunnel has been simulated. Quite detailed experimental measurements of the main combustion products and oxygen concentrations are available from these experiments. Although a scenario with a small opening was chosen the fire region did not become particularly vitiated. This is due to the fact that the size of the fire is controlled by the availability of oxygen. The highest vitiation fraction in the air entrainment region to the flame zone was about 0.20. Thus laboratory tests of more vitiated situations are needed to verify vitiation fractions higher than 0.20. In the present simulations combustion ceased when the vitiation fraction was raised to 0.40.

There seem to be very large uncertainties in measurements concerning the mass flow into the tunnel. Inflow of fresh air through the inlet pipe has been varied between 0.2 and 0.5 kg/s while outflow of fire gases from the shaft was about 2.5 kg/s according to measurements. Such a large difference indicates that there must have been a leakage somewhere through which the additional air has entered the fire compartment. The incoming air flow also exhibited pulsating behaviour, i. e. the air flow varied as a function of time between 0.2 and 0.5 kg/s. The frequency for the pulses was about 1-2 min. The gas velocities at the lower levels inside the tunnel show a reciprocated behaviour, which occurs at the same (1-2 min) frequency. This behaviour is difficult to explain. One possibility could be that due to lack of oxygen the combustion intensity has been reduced which in turn has caused the local oxygen contents near the fire to increase. Then pyrolised fuel above the fuel source has burned intensely for a short time which in turn has created a new lack of oxygen, and so on. This phenomenon is generally referred to as 'the fire breathing'.

The chemistry of combustion, especially in oxygen poor conditions is a very complicated process. The flamelet model assumes very fast chemistry and, thus, describes the flaming region best. In other regions, such as in the hot gas layer, the situation is different and is dependent on the specific location. The gas layer may contain large amounts of complete or incomplete combustion products, unburned fuel, or varying amounts of oxygen. This is due to the fact that the temperature varies throughout this region.

Thus, different physical conditions exist at different positions at any given time in a compartment fire, and one particular combustion model, while suitable for use at one location, may be unsuitable at some other location. Despite this fact, the flamelet model, as used in this study, seems to work quite well throughout the hot gas layer concerning the prediction of the gas temperature and main species concentrations.

The best results are estimated when a variable vitiation is used. The calculated temperatures in the gas layer for 15 cm below the ceiling, as a function of distance from the fire, reproduce the experimental temperatures very well. In the scenario with no vitiation the simulated temperatures are overestimated at near fire region (0-8 m) and underestimated far from the fire source. However, the slab of reinforced concrete on the ceiling was omitted in simulations, and thiscould possibly influence the simulated temperatures.

At lower levels, however, the scenario with variable vitiation gives the worst results for the simulated temperatures compared to the experimental values. This emphasises, that in order to obtain the best results in a certain part of a room fire different methods should be used. The lower level was more correctly described using the flamelet model without vitiation. The difficulty in obtaining the best results is that one would need to run both models simultaneously. To pick up the different flamelet

state relationships in each control volume would require much longer computing times and presently long execution times would be even longer, and larger computer core memory would be needed for storage of the multidimensional flamelet data tables.

In order to save computer memory and computing time a CFD code should have multi-block facilities. Such work has been done to some extent already in SOFIE and will certainly be implemented in a later version of the code. With multi-block facilities the fire source may be confined to one block in which the flamelet model with detailed chemical kinetics for different degrees of vitiation is applied. The gas layer could be separated into different blocks which could use a different chemical reaction mechanism concerning the reaction steps that mostly occur in the gas layer. The near and far fire regions of the gas layer could also be separated into different blocks, the former including faster chemical reactions for higher temperature and the latter including slow chemical reactions with considerably lower gas temperatures.

Soot calculations in this study have been conducted based on the fire gases that are assumed to flow in the gas layer. The concentrations are taken from the flamelet state relationships at the given mixture fraction value (or equivalence ratio) assumed in the inflow that penetrates the layer interface. The species in the plume flow were not seen in the flow field calculations with SOFIE, because only the main species are taken into consideration in the CFD calculations. However, the effect of all 100 species from about 2000 reaction steps are implicitly included in the flow field calculations.

The soot model in this study is based on the existence of acetylene and oxygen, see Equations (10) through (16). The concentrations of the both species together with the temperature determines the rate of formation and oxidation of soot in the gas layer.

8 Acknowledgements

This support of the Swedish Fire Research Board (BRANDFORSK) is gratefully acknowledged. The authors would like to thank Dr Fabian Mauss at Lund University, Department of Combustion Physics for calculation of Flamelets used in this study. Helpful discussions with Prof. Göran Holmstedt at Lund University, Department of Fire Technology and Docent Bror Persson at SP are also gratefully acknowledged.

9 References

[1] Tuovinen, H., "Application of Flamelet Chemistry Model to Vitiated Methane-Air Diffusion Flames", Department of Fire Safety Engineering, Lund University, Report, LUTVDG/TVBB3065-SE, 1992

[2] Tuovinen, H. "Modelling of Laminar Diffusion Flames in Vitiated Environment", 4th International Symposium on Fire Safety Science, 13-17 June 1994, Ottawa, Canada.

[3] Tuovinen, H., "CFD Modelling of Under-Ventilated Fires", Swedish National Testing and Research Institute, Fire Technology, SP- REPORT 1996:41, Borås 1996.

[4] Tuovinen, H., "CFD Modelling of Under-ventilated Fires", - and - Explosion Hazard of Substances and Venting of Deflagrations, Proceedings of the Second International Seminar. Pp 271-282, Moscow, Russia, 1997.

[5] Welch, S. , Rubini, P., SOFIE - Simulation of Fires in Enclosures, Users Quide, Cranfield University, Cranfield, UK, 1996.

[6] Lewis, M. J., Moss, J. B. And Rubini, P. A., "CFD modelling of Combustion and Heat Transfer in Compartment Fires", Fire Safety Science - Proceedings of the Fifth International Symposium, Melbourne, 1977.

[7] Bengtsson, L. G., Gustavsson, S., Tuovinen, H. and Werling, P., "Experiment at the Cardington Large Building Test Facility", Brandforsk project no 746-961, SP AR 1997:15, Borås 1997.

[8] Van Hees, P., Tuovinen, H. and Persson, B., "Simulation of the Switel Hotel Fire", Swedish National Testing and Research Institute, Fire Technology,SP-AR 1997:xx, Borås 1997.

[9] Spalding, D. B., "Mixing and Chemical Reaction in Steady Confined Turbulent Flames", *Thirteenth Symposium (International) on Combustion.* The Combustion Institute, Pittsburg, PA, pp 649-657, 1971.

[10] Magnussen, B. F., *The Eddy Dissipation Concept,* XI Task Leaders Meeting - Energy Conservation in Combustion, IEA, 1989.

[11] Liew, S. K., "Flamelet Models of Turbulent Non-Premixed Combustion". PhD thesis, Department of Aeronautics and Aerophysics, The University, Highfield, Southampton, UK,1983.

[12] Bressloff, N. W., Moss, J. B. and Rubini, P., A., "Assessment of a Differential Total Absorptivity Solution to the Radiative Transfer Equation as Applied in the Discrete Transfer Radiation Model", Numerical Heat Transfer, Part B, 29: pp 381-397, 1996.

[13] Mauss, F. And Balthasar, M., Personnel communication, Lund Institute of Technology, Department of Combustion Physics, 1997.

[14] Ingason, H., Nireus, K. and Werling, P., " Fire Tests in a Blasted Rock Tunnel", Scientific report, Defence Research Establishment, (FOA), Sweden, 1997.

[15] Kee, R. J., Miller, J. A., Jefferson, T. H., "CHEMKIN: A General - Purpose, Problem - Independent, Transportable, Fortran Chemical Kinetics Code Package", Rept. SAND80-8003, Sandia National Laboratories, Livermore, CA. 1980.

[16] Modak, A. T., "Radiation from Products of Combustion", Technical Report no. 0A0E6.BU1, Factory Mutual Research Corporation, Massachusetts, 1978.

[17] Tuovinen, H., "The computer modelling of the combustion and extinction of methane-air premixed flames by thermally stable gases" SP REPORT 1989:54.

[18] Lindstedt, R. P., Invited Lecture, 1st Specialist Meeting of the International Flame Research Foundation, Iljmuijden, 1989.

[19] Lindstedt, R. P., IUTAM Conference on Aerothermo-chemistry in Combustors, Taipei, Taiwan, 1991.

[20] Yan, Zhenghua, "Numerical Modeling of Turbulent Combustion And Flame Spread", Report LUYVDG/TVBB-1018-SE, Lund, Sweden, 1999

[21] Pitts, M. W., " The Global Equivalence Ratio Concept and the Prediction of Carbon Monoxide Formation in Enclosure Fires", Building and Fire Research Laboratory, National Institute of Standards and Technology, Gaithesburg, MD 20899, !994.

Appendix A

Chemical reaction mechanism

The chemistry of the gas layer in this study was calculated using 146 elementary step reaction mechanism involving 38 species. The reactions are of the form:

$$\sum_{i=1}^{N} v_i'\phi_i \underset{k_b}{\overset{k_f}{\leftrightarrow}} \sum_{i=1}^{N} v_i''\phi_i \qquad \text{(A1)}$$

where ϕ_i is a chemical symbol for species i, and υ'_i and $\upsilon''_i$are stoichiometric coefficients of species i appearing as reactant and product, respectively. Forward and backward reaction rates R_f and R_b are

$$R_f = k_f(\rho\sigma_m)^{\gamma_f}\prod_{i=1}^{NS}(\rho\sigma_i)^{v_i'} \qquad \text{(A2a)}$$

$$R_b = k_b(\rho\sigma_m)^{\gamma_b}\prod_{i=1}^{NS}(\rho\sigma_i)^{v_i''} \qquad \text{(A2b)}$$

where σ_m is the reciprocal of the mean molecular weight of the mixture, and γ_f and γ_b have values of unity if the reactions occur on the third body, otherwise γ_f $\gamma_b = 0$, σ_i is the number of species i, k_f and k_b are the forward and backward rate constants respectively for the reaction according to the Arrhenius expressions:

$$k_f = A_f T^{\beta_f} e^{-E_f/RT} \qquad \text{(A3a)}$$

$$k_b = A_b T^{\beta_b} e^{-E_b/RT} \qquad \text{(A3b)}$$

where E_f and E_b are the activation energies for forward and backward reactions, respectively, A_f and A_b are the Arrhenius pre-exponential factors, and β_f and β_b are the temperature exponents.

The net changes of concentration of species ϕ_i according to the reaction (A1) can be calculated from equation:

$$\frac{dC_{\phi_i}}{dt} = (v_i'' - v_i')k_f\prod_{j=1}^{N}C_{\phi_j}^{v_i'} + (v_i' - v_i'')k_b\prod_{j=1}^{N}C_{\phi_j}^{v_i''} \qquad \text{(A4)}$$

The reaction mechanism is shown in Table A1

Table A1. List of reaction mechanism used in calculation of chemistry in the hot gas layer. Total number of species in the model is 38.

	Reaction							Arrhenius parameters		
								A [mole/cm3]	β	E [cal]
1.	C2H2	+	CH	-	C3H2	+	H	.100D+15	.00000	.00000
2.	C3H2	+	H	-	C2H2	+	CH	.109D+16	.00000	35000.
3.	C3H3	+	H	-	C3H2	+	H2	500D+14	.00000	1000.0
4.	C3H2	+	H2	-	C3H3	+	H	.375D+14	.00000	23000.
5.	C3H3	+	OH	-	C3H2	+	H2O	.100D+14	.00000	.00000
6.	C3H2	+	H2O	-	C3H3	+	OH	.323D+14	.00000	36900.
7.	C3H2	+	O2	-	HCCO	+	HCO	.100D+14	.00000	.00000
8.	HCCO	+	HCO	-	C3H2	+	O2	.293D+12	.00000	55500.
9.	C2H2	+	CH	-	C3H3			.300D+14	.00000	.00000
10.	C3H3			-	C2H2	+	CH	.176D+16	.00000	.11700E+06
11.	C2H2	+	HCCO	-	C3H3	+	CO	.100D+12	.00000	2980.0
12.	C3H3	+	CO	-	C2H2	+	HCCO	.800D+12	.00000	51000.
13.	C3H3	+	O2	-	CH2CO	+	HCO	.300D+11	.00000	2870.0
14.	CH2CO	+	HCO	-	C3H3	+	O2	.169D+11	.00000	82400.
15.	C3H3	+	O	-	HCHO	+	C2H	.200D+14	.00000	.00000
16.	HCHO	+	C2H	-	C3H3	+	O	.267D+14	.00000	32500.
17.	C3H3	+	CH3	-	C2H5	+	C2H	.100D+14	.00000	37500.
18.	C2H5	+	C2H	-	C3H3	+	CH3	.855D+13	.00000	-11500.
19.	C3H4	+	H	-	C2H2	+	CH3	.200D+14	.00000	2390.0
20.	C2H2	+	CH3	-	C3H4	+	H	.331D+12	.00000	13100.
21.	C3H4	+	H	-	C3H3	+	H2	.300D+082	.0000	1000.0
22.	C3H3	+	H2	-	C3H4	+	H	.102D+072	.0000	23000.
23.	C3H4	+	OH	-	C3H3	+	H2O	.200D+082	.0000	1000.0
24.	C3H3	+	H2O	-	C3H4	+	OH	.295D+072	.0000	38000.
25.	C3H4	+	CH3	-	C3H3	+	CH4	.200D+13	.00000	7690.0
26.	C3H3	+	CH4	-	C3H4	+	CH3	.179D+13	.00000	30200.
27.	C3H4	+	C2H	-	C3H3	+	C2H2	.100D+14	.00000	.00000
28.	C3H3	+	C2H2	-	C3H4	+	C2H	.164D+13	.00000	47800.
29.	C3H4	+	O	-	C2H2	+	HCHO	.100D+13	.00000	.00000
30.	C2H2	+	HCHO	-	C3H4	+	O	.219D+12	.00000	80300.
31.	C3H4	+	O	-	C2H3	+	HCO	.100D+13	.00000	.00000
32.	C2H3	+	HCO	-	C3H4	+	O	.822D+10	.00000	29500.
33.	C3H4	+	OH	-	C2H3	+	HCHO	.100D+13	.00000	.00000
34.	C2H3	+	HCHO	-	C3H4	+	OH	.235D+12	.00000	16800.
35.	C3H4	+	OH	-	C2H4	+	HCO	.100D+13	.00000	.00000
36.	C2H4	+	HCO	-	C3H4	+	OH	.293D+12	.00000	33900.
37.	C2H	+	CH3	-	C3H3	+	H	.241D+14	.00000	.00000
38.	C3H3	+	H	-	C2H	+	CH3	.238D+15	.00000	37100.
39.	C3H6	+	O	-	C2H5	+	HCO	.360D+13	.00000	.00000
40.	C2H5	+	HCO	-	C3H6	+	O	.297D+11	.00000	29200.
41.	C3H6	+	O	-	C2H4	+	HCHO	.590D+14	.00000	5020.0
42.	C2H4	+	HCHO	-	C3H6	+	O	.392D+14	.00000	87300.
43.	C3H6	+	O	-	CH3	+	CH3CO	.500D+13	.00000	597.00
44.	CH3	+	CH3CO	-	C3H6	+	O	.102D+12	.00000	37800.
45.	C3H6	+	OH	-	C2H5	+	HCHO	.790D+13	.00000	.00000
46.	C2H5	+	HCHO	-	C3H6	+	OH	.186D+13	.00000	16500.
47.	C3H6	+	OH	-	CH3	+	CH3CHO	.510D+13	.00000	.00000
48.	CH3	+	CH3CHO	-	C3H6	+	OH	.125D+13	.00000	19800.

49.	C3H8		-	C2H5	+	CH3	.300D+23	-1.8000	88600.
50.	C2H5	+ CH3	-	C3H			8.174D+20	-1.8000	5910.0
51.	C2H2	+ C2H	-	C4H2	+	H	.300D+14	.00000	.00000
52.	C4H2	+ H	-	C2H2	+	C2H	.378D+15	.00000	26900.
53.	C4H2	+ OH	-	C2H2	+	HCCO	.150D+14	.00000	.00000
54.	C2H2	+ HCCO	-	C4H2	+	OH	.311D+13	.00000	19400.
55.	C2H2	+ C2H3	-	C4H4	+	H	.160D+14	.00000	25100.
56.	C4H4	+ H	-	C2H2	+	C2H3	.268D+15	.00000	16300.
57.	C4H4	+ C2H	-	C4H2	+	C2H3	.100D+14	.00000	.00000
58.	C4H2	+ C2H3	-	C4H4	+	C2H	.753D+13	.00000	35600.
59.	C4H4	+ OH	-	C3H3	+	HCHO	.100D+14	.00000	.00000
60.	C4H6		-	C2H3	+	C2H3	.100D-19	.00000	.00000
61.	C2H3	+ C2H3	-	C4H6			.634D-22	.00000	.10200E+06
62.	C2H3	+ C2H4	-	C4H6	+	H	.100D+12	.00000	7280.0
63.	C4H6	+ H	-	C2H3	+	C2H4	.251D+12	.00000	2090.0
64.	C4H6	+ O	-	C2H4	+	CH2CO	.100D+13	.00000	.00000
65.	C2H4	+ CH2CO	-	C4H6	+	O	.521D+13	.00000	91200.
66.	C4H6	+ O	-	HCHO	+	C3H4	.100D+13	.00000	.00000
67.	HCHO	+ C3H4	-	C4H6	+	O	.124D+14	.00000	73700.
68.	C4H6	+ OH	-	C2H5	+	CH2CO	.100D+13	.00000	.00000
69.	C2H5	+ CH2CO	-	C4H6	+	OH	.185D+13	.00000	25400.
70.	C4H6	+ OH	-	HCHO	+	C3H5	.200D+13	.00000	.00000
71.	HCHO	+ C3H5	-	C4H6	+	OH	.110D+14	.00000	34800.
72.	C4H6	+ OH	-	C2H3	+	CH3CHO	.500D+13	.00000	.00000
73.	C2H3	+ CH3CHO	-	C4H6	+	OH	.973D+13	.00000	12400.
74.	C2H6	+ H	-	C2H5	+	H2	.540D+033	.5000	5207.0
75.	C2H6	+ O	-	C2H5	+	OH	.300D+082	.0000	5111.0
76.	C2H6	+ OH	-	C2H5	+	H2O	.630D+072	.0000	645.00
77.	C2H6	+ HO2	-	C2H5	+	H2O2	.600D+13	.00000	19394.
78.	C2H6	+ CH3	-	C2H5	+	CH4	.550D+004	.0000	8288.0
79.	C2H6		-	CH3	+	CH3	.240D+17	.00000	87418.
80.	C2H4	+ H	-	C2H5			.100D+14	.00000	1505.0
81.	C2H4	+ H	-	C2H3	+	H2	.150D+15	.00000	10199.
82.	C2H4	+ O	-	CH3	+	HCO	.160D+101	.2000	740.00
83.	C2H4	+ OH	-	C2H3	+	H2O	.300D+14	.00000	2986.0
84.	C2H4	+ CH3	-	C2H3	+	CH4	.420D+12	.00000	11106.
85.	C2H5		-	C2H4	+	H	.200D+14	.00000	39648.
86.	C2H5	+ O2	-	C2H4	+	HO2	.200D+13	.00000	4992.0
87.	C2H5	+ H	-	CH3	+	CH3	.300D+14	.00000	.00000
88.	C2H5	+ C2H5	-	C2H6	+	C2H4	.140D+13	.00000	.00000
89.	C2H3	+ O2	-	C2H2	+	HO2	.100D+13	.00000	.00000
90.	C2H3	+ H	-	C2H2	+	H2	.200D+14	.00000	.00000
91.	C2H3	+ O	-	C2H2	+	OH	.300D+14	.00000	.00000
92.	C2H2	+ H	-	C2H3			.550D+13	.00000	2412.0
93.	C2H2	+ O	-	CH2	+	CO	.410D+091	.5000	1696.0
94.	C2H2	+ OH	-	CH2	+	HCO	.300D+13	.00000	1099.0
95.	C2H2	+ O2	-	HCO	+	HCO	.400D+13	.00000	28000.
96.	CH4	+ H	-	CH3	+	H2	.220D+053	.0000	8742.0
97.	CH4	+ O	-	CH3	+	OH	.120D+082	.1000	7619.0
98.	CH4	+ OH	-	CH3	+	H2O	.160D+072	.1000	2460.0
99.	CH4	+ HO2	-	CH3	+	H2O2	.200D+12	.00000	14940.
100.	CH4		-	CH3	+	H	.100D+16	.00000	.10032E+06
101.	CH3	+ O2	-	HCHO	+	H + O	.150D+14	.00000	28662.
102.	CH3	+ H2	-	CH4	+	H	.660D+033	.0000	7739.0

103.	CH3	+	M	-	CH2	+	H	.100D+17	.00000	90523.
104.	CH3	+	H	-	CH4			.600D+17	-1.0000	.00000
105.	CH3	+	O	-	HCHO	+	H	.700D+14	.00000	.00000
106.	CH3	+	CH3	-	C2H6			.240D+15	-.40000	.00000
107.	CH3	+	CH3	-	C2H5	+	H	.800D+15	.00000	26512.
108.	CH3	+	CH3	-	C2H4	+	H2	.100D+17	.00000	32005.
109.	CH2	+	O2	-	CO2	+	H + H	.130D+14	.00000	1505.0
110.	CH2	+	O	-	CO + H	+	H	.500D+14	.00000	.00000
111.	CH2	+	CH3	-	C2H4	+	H	.400D+14	.00000	.00000
112.	HCHO	+	H	-	HCO	+	H2	.250D+14	.00000	3989.0
113.	HCHO	+	O	-	HCO	+	OH	.350D+14	.00000	3511.0
114.	HCHO	+	OH	-	HCO	+	H2O	.300D+14	.00000	1194.0
115.	HCHO	+	HO2	-	HCO	+	H2O2	.100D+13	.00000	8000.0
116.	HCHO	+	CH3	-	CH4	+	HCO	.100D+12	.00000	6091.0
117.	HCHO	+	M	-	HCO	+	H + M	.500D+17	.00000	76431.
118.	HCO	+	O2	-	CO	+	HO2	.300D+13	.00000	.00000
119.	HCO	+	M	-	CO	+	H + M	.250D+15	.00000	16791.
120.	HCO	+	H	-	CO	+	H2	.200D+15	.00000	.00000
121.	HCO	+	O	-	CO	+	OH	.300D+14	.00000	.00000
122.	HCO	+	O	-	CO2	+	H	.300D+14	.00000	.00000
123.	HCO	+	OH	-	CO	+	H2O	.500D+14	.00000	.00000
124.	CO	+	OH	-	CO2	+	H	.440D+071	.5000	-740.00
125.	CO	+	HO2	-	CO2	+	OH	.150D+15	.00000	23574.
126.	CO	+	O2	-	CO2	+	O	.250D+13	.00000	47769.
127.	H2O2	+	H	-	H2	+	HO2	.170D+13	.00000	3750.0
128.	H2O2	+	H	-	H2O	+	OH	.100D+14	.00000	3583.0
129.	H2O2	+	O	-	HO2	+	OH	.280D+14	.00000	6401.0
130.	H2O2	+	OH	-	HO2	+	H2O	.700D+13	.00000	1433.0
131.	H2O2	+	M	-	2OH	+	M	.120D+18	.00000	45381.
132.	H2	+	O	-	OH	+	H	.150D+082	.0000	7548.0
133.	H2	+	OH	-	H2O	+	H	.100D+091	.6000	3296.0
134.	H2	+	HO2	-	H2O2	+	H	.730D+12	.00000	18654.
135.	HO2	+	H	-	OH	+	OH	.150D+15	.00000	1003.0
136.	HO2	+	H	-	H2	+	O2	.250D+14	.00000	693.00
137.	HO2	+	O	-	O2	+	OH	.200D+14	.00000	.00000
138.	HO2	+	OH	-	H2O	+	O2	.200D+14	.00000	.00000
139.	HO2	+	HO2	-	H2O2	+	O2	.200D+13	.00000	.00000
140.	H	+	H2O	-	H2	+	OH	.460D+091	.6000	18558.
141.	H	+	O2	-	OH	+	O	.120D+18	-.91000	16504.
142.	H	+	O2	+	M- HO2	+	M	.200D+19	-.80000	.00000
143.	OH	+	H	-	H2	+	O	.680D+072	.0000	5570.0
144.	OH	+	OH	-	H2O	+	O	.150D+101	.1400	.00000
145.	O	+	H2O	-	OH	+	OH	.150D+111	.1400	17245.
146.	O	+	OH	-	O2	+	H	.180D+14	.00000	.00000

SP Swedish National Testing and Research Institute
Box 857, SE-501 15 BORÅS, Sweden
Telephone: +46 33 16 50 00, Telefax: +46 33 13 55 02
E-mail: info@sp.se, Internet: www.sp.se

SP REPORT 1999:03
ISBN 91-7848-757-9
ISSN 0284-5172